JOURNAL OF VIROLOGY, Mar. 2006, p. 2797–2807 Vol. 80, No. 6
0022-538X/06/$08.00+0 doi:10.1128/JVI.80.6.2797–2807.2006

Immune Suppression Uncovers Endogenous Cytopathic Effects of the Hepatitis B Virus

Philip Meuleman,[1] Louis Libbrecht,[2] Stefan Wieland,[3] Rita De Vos,[2] Nagy Habib,[4] Anna Kramvis,[5] Tania Roskams,[2] and Geert Leroux-Roels[1]*

Center for Vaccinology, Ghent University and Hospital, Building A, First Floor, De Pintelaan 185, B-9000 Ghent, Belgium[1]; Department of Morphology and Molecular Pathology, U.Z.-K.U. Leuven, Minderbroederstraat 12, B-3000 Leuven, Belgium[2]; Department of Molecular and Experimental Medicine, The Scripps Research Institute, La Jolla, California 92037[3]; Department of Surgery, Faculty of Medicine, Imperial College, Hammersmith Hospital Campus, London, United Kingdom[4]; and Molecular Hepatology Research Unit, Department of Medicine, University of the Witwatersrand, Johannesburg, South Africa[5]

Received 3 August 2005/Accepted 27 December 2005

It is generally accepted that the host's immune response rather than the virus itself is causing the hepatocellular damage seen in acute and chronic hepatitis B virus (HBV) infections. However, in situations of severe immune suppression, chronic HBV patients may develop a considerable degree of liver disease. To examine whether HBV has direct cytopathic effects in severely immune compromised hosts, we have infected severe combined immune deficient mice (uPA-SCID), harboring human liver cells, with HBV. Serologic analysis of the plasma of HBV-infected animals revealed the presence of extremely high amounts of viral genomes and proteins. Histological analysis of the livers of uPA-SCID chimeras infected with HBV for more than 2 months showed that the majority of human hepatocytes had a ground-glass appearance, stained intensely for viral proteins, and showed signs of considerable damage and cell death. This histopathologic pattern closely resembles the picture observed in the livers of immunosuppressed HBV patients. These lesions were not observed in animals infected with HBV for less than 1 month. Ultrastructural analysis of long-term-infected hepatocytes showed a highly increased presence of cylindrical HBsAg structures, core particles, and Dane particles compared to short-term-infected hepatocytes. These long-term-infected hepatocytes also contained elevated amounts of HBV cccDNA. In conclusion, HBV causes dramatic intracellular changes and hepatocellular damage in the human hepatocytes that reside in a severely immune deficient mouse. These lesions show much resemblance to the ones encountered in immunosuppressed chronic HBV patients. Our observations indicate that HBV may be directly cytopathic in conditions of severe immune suppression.

Hepatitis B virus (HBV) is considered to be a noncytopathic virus, and the hepatocellular damage observed during acute and chronic HBV infections is thought to be mediated by the host's immune response to the virus (6). More than 90% of immune competent adults who become infected with HBV display a vigorous, polyclonal, and multispecific antiviral immune response that results in a rapid reduction of the viral load and a long-lasting, protective immunity. About 5% of infected immune competent adults and a large proportion of neonates (up to 90%) and young children are unable to mount an immune response of sufficient magnitude and complexity to clear the virus and develop a chronic infection with various degrees of necro-inflammatory liver disease. Self-limiting and chronic HBV infections represent different stages of a dynamic equilibrium between the immune response of the host and the replicative capacity of the virus.

Suppression of the immune system by immunosuppressive agents or by progressive immune failure in the context of acquired immune deficiencies (e.g., human immunodeficiency virus/AIDS) may lead to reactivation of seemingly recovered or "silent" HBV infections (1). This generally presents as a reappearance of "classic" HBV markers such as HBsAg, HBeAg, and HBV DNA, in the absence of overt liver disease and/or elevated levels of transaminases. In addition, chronic HBV carriers who undergo an immunosuppressive therapy for an autoimmune disorder (62) or after liver (3, 11, 32), renal (5, 27), or bone marrow (43) transplantation or who are treated with chemotherapy for non-Hodgkin lymphoma (39) experience increased viremia accompanied by intensified viral protein expression in the infected hepatocytes. In a minority of these immunosuppressed patients, this liver disease may evolve toward fibrosing cholestatic hepatitis (FCH), an aggressive and mostly fatal form of viral hepatitis. FCH is associated with increased viral replication (42) and is characterized histologically by high intrahepatic expression of viral proteins, diffuse hepatocyte ballooning, the presence of ground-glass hepatocytes, prominent cholestasis, and periportal fibrosis (3, 5, 11, 27, 32, 42).

To examine whether this particular disease course is related to the severe immunosuppression encountered in these patients, we have studied the evolution of an experimental HBV infection in the human liver-uPA-SCID model (46). This model is based on the successful transplantation of uPA mice (24, 51, 52), backcrossed on the immune deficient SCID mouse, with primary human hepatocytes. We have recently shown that, after transplantation, up to 85% of the liver of these chimeric animals is repopulated by well-organized hu-

* Corresponding author. Mailing address: Center for Vaccinology, Ghent University and Hospital, Building A, First Floor, De Pintelaan 185, 9000 Ghent, Belgium. Phone: 32 9 240 34 22. Fax: 32 9 240 63 11. E-mail: geert.lerouxroels@UGent.be.

man hepatocytes that retain their normal cell functions and characteristics (46).

In addition, we compared the changes induced by HBV in this animal model with immunohistochemical and ultrastructural observations made in liver biopsies of an immunosuppressed patient with HBV-induced FCH and with literature data on this syndrome.

We show that HBV infection of human hepatocytes in immune deficient uPA mice induces a clinicopathological syndrome that closely resembles the picture in severely immunodepressed chronic HBV patients, which indicates that the hepatocellular damage in these HBV patients is caused by endogenous cytopathic effects of the virus itself.

MATERIALS AND METHODS

Patient with HBV-induced FCH. In the present study, we have examined histologically a needle liver biopsy and fragments from the explant liver of a patient with HBV-induced FCH. The patient was a 54-year-old female chronic hepatitis B carrier who developed hemolytic-uremic syndrome, possibly induced by a severe, acute gastroenteritis. She was treated with plasmaferesis, hemodialysis, and corticosteroids and intermittently with vincristine and cyclosporine. The immunosuppressive treatment elicited a FCH, which was confirmed by needle liver biopsy. Treatment with lamivudine could not prevent the development of subacute liver failure, and the patient underwent a liver transplantation.

Production of human liver-uPA-SCID mice and infection with HBV. Human hepatocytes were isolated via a standard collagenase digestion (46) from tumor-free liver fragments, collected from three patients undergoing a partial hepatectomy. All patients gave written, informed consent, and the study protocol was approved by the Ethical Committee of the Ghent University Hospital. Within 2 weeks after birth, nine homozygous uPA-SCID mice (47) were transplanted with one million human hepatocytes (three mice with donor 1 hepatocytes, four mice with donor 2 hepatocytes, and two mice with donor 3 hepatocytes). At selected moments, plasma was taken and stored at −80°C until analysis. To evaluate graft take and survival, human albumin was determined by using an in-house enzyme-linked immunosorbent assay (46).

Five weeks after the transfer of hepatocytes and the demonstration of successful engraftment, these nine chimeric mice were infected with HBV via an intraperitoneal injection of 100 μl of serum from a patient that was suffering from a mild chronic hepatitis B infection for at least 17 years. This serum contained 10^7 copies of HBV DNA/ml and was positive for HBsAg and HBeAg and negative for anti-HBs and antibodies against HCV, HDV, and human immunodeficiency virus.

Detection and quantification of viral DNA, HBsAg, and HBeAg. HBV DNA levels in mouse EDTA plasma were quantified by using the Cobas Amplicor HBV Monitor test (Roche Diagnostics, Mannheim, Germany). HBsAg and HBeAg levels were measured with a modified protocol of the Axsym HBsAg V2 and the Axsym HBe 2.0 system (Abbott, Chicago, Ill.), respectively. Internal calibration panels, standardized to the NIBSC HBsAg standard (international units [IU]/ml) and to the Paul Ehrlich Institute standard for HBeAg (Paul Ehrlich Institute units [PEIU]/ml), were serially diluted to generate two calibration curves of fluorescence rate versus concentration. The concentrations of HBsAg and HBeAg in plasma samples were determined by interpolation of the fluorescence rate on 5-point and 7-point calibration curves, respectively.

UPA-SCID mice livers used for histopathological evaluation. The livers of seven uPA-SCID mice were used for extensive histopathological evaluation. Two HBV-infected animals were sacrificed 21 and 25 days after inoculation and are referred to here as "short-term infected," whereas two other infected animals were sacrificed 73 and 88 days after infection. These animals are referred to as "long-term infected." The liver pathology in these livers was compared to that in a 2-week-old untransplanted, uninfected uPA-SCID mouse and that in two chimeric mice 36 and 78 days after transplantation with human hepatocytes. The latter animals were not inoculated with HBV.

Preparation of tissues for histological study. The largest fragment of each mouse liver was fixed in either B5-fixative or 6% formalin and then embedded in paraffin. A small part of each fresh liver was fixed in 2.5% glutaraldehyde–0.1 M phosphate buffer and prepared for standard electron microscopy. The remainder was snap-frozen in liquid nitrogen-cooled isopentane and stored at −80°C until further use.

The largest part of the needle biopsy of an FCH patient was fixed in B5 fixative and embedded in paraffin. Small fragments were snap-frozen or fixed in glutaraldehyde for electron microscopy. Five large biopsies were randomly taken from the explant liver and embedded in paraffin after fixation in 6% formalin. Small fragments were snap-frozen or fixed in glutaraldehyde for electron microscopy.

Histology. Four-micrometer-thick sections from paraffin-embedded liver tissue were stained with hematoxylin and eosin (H&E) for overall histopathological evaluation, periodic-acid-Schiff (PAS) to assess cellular polysaccharide deposits, PAS after predigestion with amylase (PASα) to detect ceroid macrophages, Sirius red for fibrosis, and Hall-Van Gieson to detect bilirubinostasis (2, 40, 41). Five-micrometer-thick sections from frozen liver tissue were fixed in acetone for 10 min after overnight drying, followed by an oil red O (ORO) staining to visualize steatosis (2).

Immunohistochemistry. Four-micrometer-thick sections from paraffin-embedded tissue were deparaffinized and rehydrated. Incubation with the primary antibodies was performed at room temperature for 30 min, followed by a wash in three changes of phosphate-buffered saline for 5 min. The primary antibodies used to detect and study the different cell types of human liver within the mouse livers were as follows: a polyclonal rabbit antibody to human albumin (dilution 1/200; Dako, Denmark) and monoclonal mouse antibodies to human hepatocytes (hepatocyte paraffin 1 or Heppar-1, dilution 1/50; Dako), mitochondria (clone 113-1, dilution 1/100; Chemicon), pan-cytokeratin (clone KL1, dilution 1/50; Immunotech), cytokeratin 8 (CK8; clone 35betah11, dilution 1/100; Dako), CK18 (clone CD10, dilution 1/10; Dako), CK7 (clone OV-TL12/30, dilution 1/50; Dako), and CK19 (clone RCK108, dilution 1/20; Dako). The antibodies to albumin and Heppar-1 are well-established markers of hepatocytes (59). The different anti-keratin antibodies were used to detect all human epithelial cells. Their staining intensity and pattern and the morphology of the positive cells makes it possible to recognize mature hepatocytes, bile duct epithelial cells, and cells of the progenitor cell compartment (i.e., hepatic progenitor cells, intermediate hepatocyte-like cell and reactive ductular cells) (37). Expression of viral proteins was assessed by using a polyclonal rabbit antibody to HBcAg (dilution 1/200; Dako) and monoclonal mouse anti-human antibodies to HBsAg (clone H1, dilution 1/80; ForLab, Belgium). The monoclonal mouse anti-human antibody Ki67 (clone Mib-1, dilution 1/100; Dako) was used to assess the proliferative status of human hepatocytes (20). To evaluate both human and mouse cells, polyclonal rabbit antibodies against human cytokeratins (dilution 1/20; Dako) and CEA (dilution 1/300; Dako) were used (15, 36). The polyclonal antibody to CEA is a marker for canaliculi (33). For all mouse monoclonal antibodies and the rabbit polyclonal anti-cytokeratin antibody, the secondary antibodies were undiluted anti-mouse and anti-rabbit Envision (Dako), respectively. Sections wherein the incubation with the first and/or secondary/tertiary antibodies were omitted, and fully processed sections of liver tissue from untransplanted animals served as controls. Positive controls consisted of selected liver biopsies from the clinical routine that were stained with these antibodies.

Quantitative assessment of the different human liver cell types present in uPA-SCID liver. To measure the fraction of liver parenchyma represented by human hepatocytes, digital pictures (total of seven to eight pictures per liver) were taken with a ×5 objective lens. Using Adobe Photoshop 7.0, the number of pixels within the total liver parenchyma (excluding large portal veins, areas of calcifications, red foci, and areas without tissue) was determined and compared to the number of pixels within delineated human hepatocyte areas. To quantify proliferating hepatocytes, the number of Ki67 nucleus-positive hepatocytes was counted in random fields containing at least 300 human hepatocytes.

HBV genotyping and sequencing. Total DNA from the infecting inoculum and from mouse plasma was extracted by using the QIAamp DNA Minikit (QIAGEN GmbH, Hilden, Germany) according to the manufacturer's instructions. The HBV isolates were genotyped by using the method of Lindh et al. (38). Primers P7 and P8 were used to amplify nucleotides (nt) 256 to 796 of the S region. The amplicon was then cleaved by using restriction enzymes HinfI and Tsp509I, in separate reactions to give the characteristic restriction fragment length polymorphism patterns for the different genotypes.

The full sequence of the HBV strains was obtained by amplifying overlapping regions of the genome as follows: (i) with a single-round PCR with the primer pairs P7 and P8 (nt 230 to 796) (38), 455(+) and 1800(−) (29), and 2408(+) and 1327(−) (49); (ii) with a nested PCR with primer pairs 1689(+) and 2498(−) for the first round (I) and 1898(+) and 2396(−)for the second round (II) (49), 1689(+) and 685(−) (I) and 2267(+) and 2858(−) (II), and 1730(+) and 2043(−) (I) and 1763(+) and 1966(−) (II) (49). The amplicons were prepared for direct sequencing by using the BigDye Terminator v3.0 Cycle Sequencing Ready Reaction Kit (Applied Biosystems, Foster City, Calif.) and sequenced on a Spectrumedix SCE2410 (SpectruMedix LLC, Pennsylvania). In addition to the primers used for amplification, HBV-specific primers [112(+), 970(+), 1373(+), 2807(+), 472(−), 1009(−), 1920(+) (5′-ATT TGG AGC TAC TGT GGA G-3′),

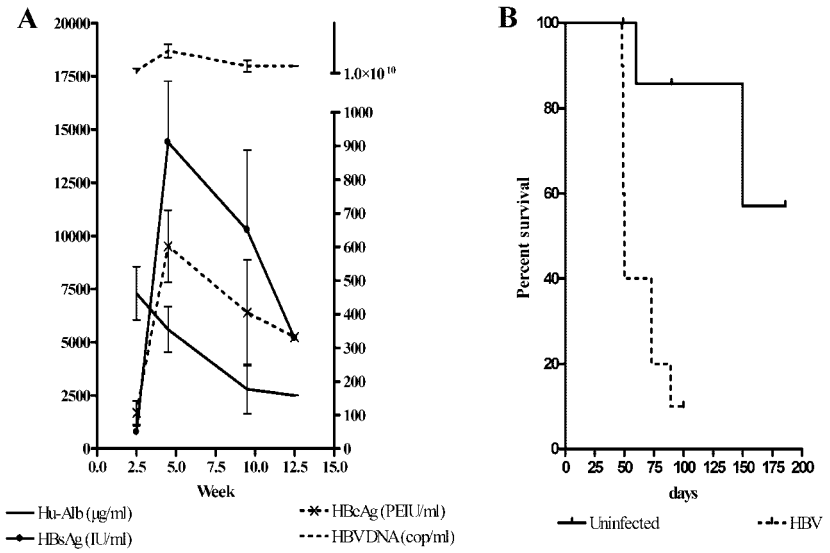

FIG. 1. (A) Overview of plasma analysis of 6 HBV-infected human liver-uPA-SCID mice. The concentration of human albumin (Hu-Alb) and HBsAg can be deduced from the left axis, while HBeAg and HBV DNA concentrations can be derived from the right axis. In general, all HBV markers (HBsAg, HBeAg, and HBV DNA) increased up to 5 weeks after infection. Later on, the concentrations of viral proteins dropped impressively and coincided with a drastic decrease in secreted human albumin. The drop in viral proteins is also accompanied with a reduction in produced virions. (B) Kaplan-Meier graph illustrating the survival of human liver-uPA-SCID mice. HBV-infected animals show a significantly shorter life span compared to uninfected counterparts.

and 2352(−) (5′-TCT AAC AAC AGT ATT CTC-3′)] were used for sequencing. All sequences were analyzed in both the forward and reverse directions. Complete HBV genome sequences were compared to corresponding sequences of HBV from GenBank.

HBV RNA detection in the liver. Frozen liver tissues were dissolved in guanidine-isothiocyanate solution, and RNA was extracted by the acid-guanidinium phenol-chloroform method (8). Total RNA (10 μg) was analyzed by Northern blotting and probing for HBV and GAPDH exactly as described previously (21).

HBV DNA detection in the liver. Total liver DNA was extracted from frozen liver biopsy samples as described previously (22), and the levels of HBV DNA replicative intermediates were determined by quantitative real-time PCR using a Bio-Rad iCycler system exactly as described previously (56).

HBV cccDNA quantification in the liver. Covalently closed circular DNA (cccDNA) was isolated from frozen liver biopsies and analyzed by Southern blotting and by quantitative real-time PCR for quantification exactly as described previously (60). For quantification of mitochondrial DNA derived from the human hepatocytes, the following primers specific for human mitochondrial DNA were used: HsMito3362U, 5′-TCCTAATGCTTACCGAACGA-3′; and HsMito3442L, 5′-GCGTCAGCGAAGGGTTGTAG-3′. The number of human hepatocytes represented in the total DNA samples was determined by quantitative real-time PCR of total liver DNA for the cellular gene IMAP1 (30) using primers specific for the human IMAP gene: hIMAP3652U, 5′-TTTTCAGCT CCCAAGTGTCC-3′; and hIMAP3703L, 5′-GCCGAGAGCAGGTAGCAGT-3′, and human genome copy numbers were obtained by comparing the IMAP PCR results with a dilution series of purified genomic human DNA (Clontech, Mountain View, CA) under the assumption that ~6-pg genomic DNA represent one hepatocyte.

Statistics. Statistical analysis was performed by using GraphPad Prism v4. Before regression analysis, the normality of distribution of HBsAg, HBeAg, HBV DNA, and albumin was assessed by the Kolmogorov-Smirnov test. Survival curves were created by using Kaplan-Meier analysis.

RESULTS

Hepatocyte transplantation and engraftment. Nine uPA-SCID mice, successfully transplanted with primary human hepatocytes, were infected with 10^6 HBV genome copies. Seventeen days later, EDTA plasma was analyzed for the presence of HBsAg, HBeAg, and HBV DNA. Eight of the nine animals were positive for these viral markers. The one negative animal showed signs of infection 2 weeks later, when HBsAg, HBeAg, and HBV DNA appeared in the plasma.

Kinetic study of HBV markers. To study the progression of the HBV infections in uPA-SCID mice, we quantified the viral proteins and DNA in the mouse plasma. Figure 1A shows the evolution of the virologic parameters, together with the human albumin levels, obtained in six mice and shows that 2.5 weeks after injection of HBV the mean HBV DNA titer was 1.4×10^{10} copies/ml, while HBeAg and HBsAg reached levels of 107 PEIU/ml and 788 IU/ml, respectively. Serologic HBV parameters peaked between 4 and 5 weeks after infection and reached a mean HBV DNA level of 5×10^{10} copies/ml, a mean HBeAg level of 602 PEIU/ml, and a mean HBsAg level of 14,398 IU/ml. From then on three animals appeared clinically sick and died within 2 weeks. One month later, the surviving animals had either equal or lower HBeAg and HBsAg levels, and all had lower HBV DNA levels in their plasma. The clinical condition of two animals rapidly deteriorated, and they died 4 days later. Only one mouse survived beyond 12.5 weeks after infection. In all animals, clinical deterioration coincided with a dramatic drop of human albumin levels in plasma. The median life span of the HBV-infected animals was 50 days after infection or 85 days after transplantation. This is significantly shorter ($P < 0.0001$) than the survival of uninfected mice (Fig. 1B), which survived for at least 220 days after transplantation and maintained a human albumin concentration in their plasma ranging between 4 and 6 mg/ml.

Correlation between HBV DNA and viral proteins. When HBsAg levels were compared to the levels of HBeAg in the plasma of the infected animals, a strong and linear correlation was observed ($r = 0.9808$, $P < 0.0001$) (Fig. 2A). Figure 2B shows a linear correlation between HBV DNA and both HBsAg ($r =$

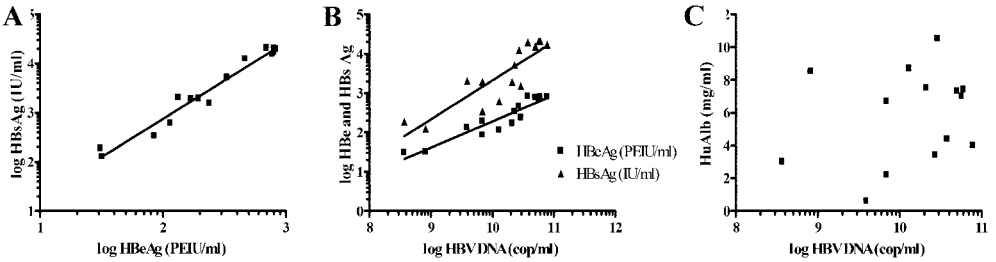

FIG. 2. (A and B) Plasma analysis of HBV-infected animals revealed linear correlations between HBsAg and HBeAg ($r = 0.9808$, $P < 0.0001$) (A) and between HBV DNA and HBsAg ($r = 0.8710$, $P < 0.0001$) and HBeAg ($r = 0.9344$, $P < 0.0001$) (B). (C) In contrast, no correlation between any viral marker and human albumin (HBV DNA and human albumin, $r = 0.244$, $P = 0.4006$) could be demonstrated.

0.8710, $P < 0.0001$) and HBeAg ($r = 0.9344$, $P < 0.0001$). The absence of any correlation between the human albumin levels and the HBV markers (Fig. 2C) indicates that the correlations highlighted before are specific for viral protein expression and replication.

Sequence analysis of HBV. The HBV strains amplified from the infecting inoculum and from the mouse plasma (88 days after inoculation) both belonged to genotype E, serological subtype *ayw4*. The complete genomes of the two HBV isolates were sequenced and compared by phylogenetic analysis to the 17 complete sequences of genotype E in the GenBank database (AB091255, AB091256, AB032431, X75657, X75664, AB106564, AY738144, AY739675, and DQ060822 to DQ060830 (A. Kramvis et al., submitted for publication, and data not shown). Both isolates had a genome length of 3,212 nt characteristic of genotype E, and their sequences were identical (GenBank accession no. AY935700).

The pre-S1 sequence was completely conserved, whereas a single missense mutation relative to other genotype E sequences was found in the pre-S2: T53C (Phe22Leu). The polymerase open reading frame (ORF) was well conserved relative to other genotype E sequences except for an amino acid substitution within the reverse transcriptase rtSer212Thr as a result of the T766A missense mutation. The following missense mutations were detected in the X ORF overlapping the basic core promoter: T1753C (Ile127Thr), A1762U (Lys130Met), and G1764A (Val131Ile). The core region contained four missense mutations: A2092T (Glu64Asp), C2093G (Leu65Val), A2099T (Thr67Ser), and A2159G (Ser87Gly).

Histology. The histological findings of the livers from uninfected, short-term HBV-infected and long-term HBV-infected animals are hereafter described in this order. However, we present the figures of short-term and long-term-infected animals side to side to illustrate the differences between both conditions in the best way. For this reason, the order of figures does not always follow the flow of the text.

Histologic analysis of the livers of transplanted, uninfected uPA-SCID mice. At 36 and 78 days after transplantation, the livers of two uninfected animals were examined. Mature human hepatocytes could easily be recognized because they are larger in size than their murine counterparts and, in addition, they stained positive for Heppar-1, human albumin, mitochondria, and CK8/18. All of these markers were negative on tissue derived from untransplanted control animals. We recently found (46) that the human hepatocytes tend to accumulate glycogen in the cytoplasm, which results in the typical "plant-like" morphology that is also seen in all glycogen storage diseases, except in type IV. Steatosis of human hepatocytes was minimal. At 25 days after transplantation, one-quarter of the liver parenchyma was occupied by nodules of human hepatocytes. Ki67 staining showed that 18% of human cells were proliferating. In contrast to the sick mouse liver parenchyma, the regions occupied by human hepatocytes contained almost no ceroid macrophages. At 73 days after transplantation, 66% of the liver parenchyma was of human origin. Only 6% of human cells were still proliferating, and ceroid macrophages were still rare within the human zones. Except for glycogen storage, human hepatocytes showed no abnormalities. Besides mature hepatocytes, the host liver also contained human hepatic progenitor cells, which were recognized on the basis of their characteristic morphology and immunohistochemical phenotype (37).

Histologic and ultrastructural analysis of the liver of short-term-infected animals. Two uPA-SCID mice, transplanted with human hepatocytes and subsequently infected with HBV, were sacrificed 21 and 25 days after infection. Figure 3A shows that also in this animal and in no way different from the livers of noninfected mice, human hepatocytes were excessively loaded with glycogen and formed large areas occupying 34 and 87% of mouse liver parenchyma, respectively. Apart from the glycogen storage, no other signs of damage or cell loss were seen. The human hepatocytes stained strongly for human albumin (Fig. 3B), and ceroid macrophages were confined to the mouse areas (Fig. 3C). Hepatocytes staining for Ki67 were scattered over the liver and accounted for 10% of all human hepatocytes. There were no human hepatocytes with a "ground-glass" aspect of the cytoplasm.

Figure 4A shows that 25 days after infection almost all human hepatocytes stained for HBcAg, displaying a strong signal in the nucleus and a moderate one in the cytoplasm. At 21 days after infection, 50% of the human hepatocytes stained positive (not shown). The cytoplasm of the human hepatocytes almost always had a granular staining for HBsAg, frequently with an accentuation near the cell membrane (Fig. 4B). Whereas almost all human hepatocytes stained positive for HBsAg 25 days after inoculation, only 10% stained positive 21 days after infection. The staining patterns and intensities are similar to those observed in liver biopsies of patients with chronic HBV in the viral replicative phase. The number of positive hepatocytes is usually lower in human liver biopsies (14).

In addition to human hepatocytes and diseased mouse hepatocytes, seven red foci (mouse regenerative nodules that have

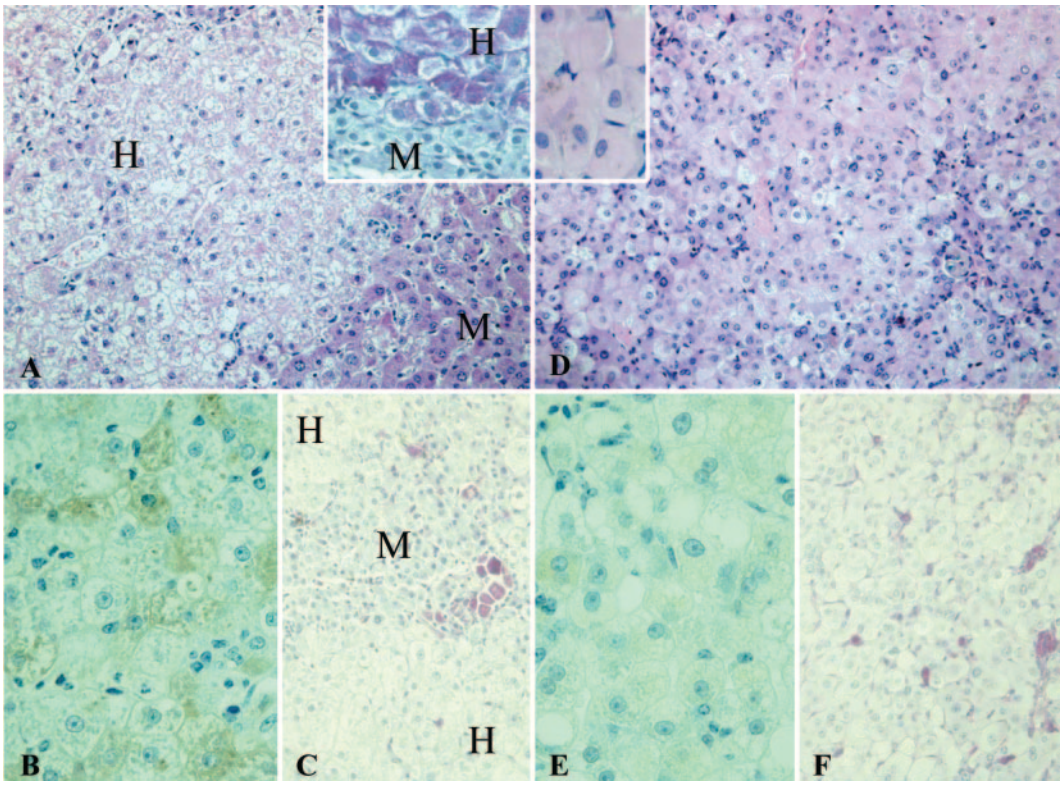

FIG. 3. Comparison of liver architecture of short-term (A, B, and C) and long-term (D, E, and F) HBV-infected human liver-uPA-SCID mice. Human hepatocytes (H) in short-term-infected animals have a pale appearance on H&E staining (A) due to the accumulation of glycogen as shown by PAS staining (inset). Diseased mouse hepatocytes (M) are devoid of glycogen. (B) Staining for human albumin shows that short-term infection does not compromise the functionality of the human hepatocytes. (C) PASα staining on the same livers shows that ceroid macrophages, an indication of cell loss, are confined to the diseased mouse regions. (D) The majority of long-term HBV-infected human hepatocytes have a ground-glass appearance on H&E staining, whereas these were absent in uninfected and short-term-infected livers. The insert shows a magnification of human ground-glass hepatocytes. (E) Long-term HBV infection results in an overall deterioration of the condition of the cells as shown by the decreased albumin production. (F) Large amounts of ceroid macrophages are now also present in the regions occupied by human hepatocytes, indicating that long-term infection causes the death of human hepatocytes. Original magnifications: A, C, D, and F, ×200; insets, B, and E, ×400.

deleted the uPA transgene) were also present in the liver of one short-term-infected animal. These consisted of 21 to 88 hepatocytes that were partly or completely surrounded by areas of human hepatocytes. The interface between red foci and human areas was neither sharply delineated nor compressed, and the two cell types seemed to infiltrate each other's "territories." These findings suggest that the human hepatocytes and the transgene-free mouse hepatocytes are responding equally well to the available growth stimuli. As in noninfected mouse livers, human hepatic progenitor cells and intermediate hepatocyte-like cells were focally present at the human-mouse parenchymal interface.

Using electron microscopy, noncoated viral particles with a diameter of 21 to 24 nm, corresponding to HBV core particles, could be observed dispersed in the nuclei of several human hepatocytes. In the cisternae of the endoplasmic reticulum, one or two longitudinally transected tubules and cross-sectioned spheres of HBsAg were present. In some cisternae, core particles, surrounded by a clear halo and a dark ring approximately 40 nm in size, corresponding to Dane particles were observed. In addition to the presence of viral and subviral particles, no ultrastructural alterations could be observed in these hepatocytes compared to those of noninfected animals.

Histologic and ultrastructural analysis of the livers of long-term-infected animals. The clinical condition of the HBV-infected animals deteriorated over time, and some animals died spontaneously. Two mice that looked clinically "terminal" (infected for 73 and 88 days) were sacrificed to examine their livers. In these mice, the cytoplasm of most human hepatocytes had a "ground-glass" appearance (Fig. 3D) and no longer showed the excessive accumulation of glycogen, observed in uninfected or short-term-infected mice. The stainings for CK8, CK18, pan-cytokeratin, albumin, Heppar-1, and mitochondria were diffusely positive in most human hepatocytes. The intensity of the staining for albumin was much weaker compared to the four other markers (Fig. 3E). This was not the case in the short-term-infected livers (Fig. 3B). Small areas of diseased mouse liver parenchyma were separated from each other by large areas of human hepatocytes that occupied 70% (73 days postinfection) and 50% (88 days postinfection) of the liver parenchyma. Within the human parenchyma, scattered ceroid macrophages were seen that sometimes formed small clusters (Fig. 3F), indicating considerable loss and damage of human hepatocytes. Occasionally, degenerative and apoptotic hepatocytes were observed, but never signs of bilirubinostasis. In a complete section, only five human hepatocytes were Ki67 positive,

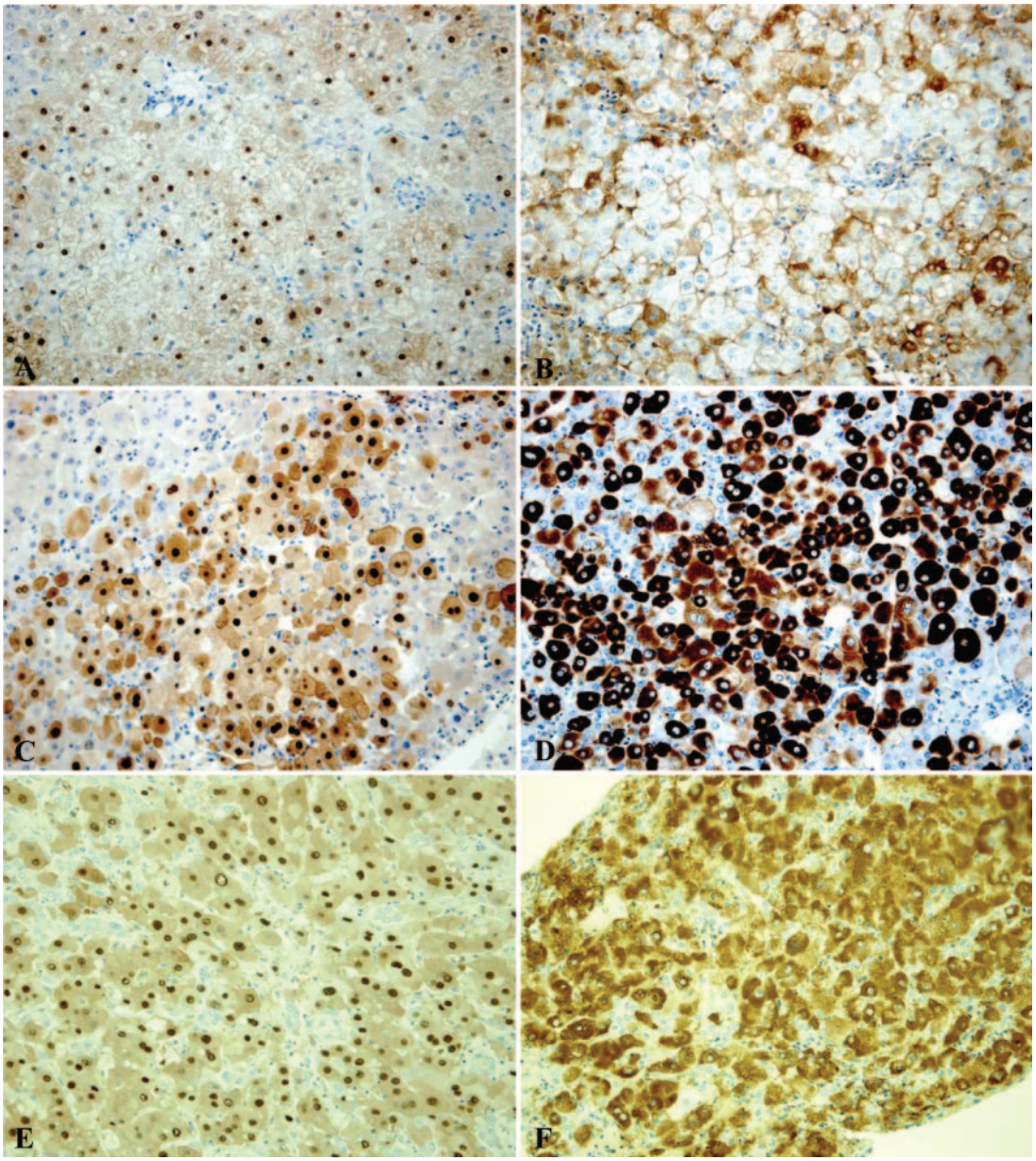

FIG. 4. Immunohistochemical staining for HBcAg (A, C, and E) and HBsAg (B, D, and F) on liver sections of short-term (upper panel) and long-term (middle panel) HBV-infected human liver-uPA-SCID mice and biopsies from a patient suffering from FCH (lower panel). We can clearly observe a highly increased presence and difference in the distribution of both viral proteins in long-term-infected tussue compared to short-term-infected tissue. The amount and pattern of HBcAg and HBsAg staining on the long-term-infected liver corresponds very well to the one observed in liver tissue derived from the FCH patient. Original magnifications, ×200.

which is much less than in the uninfected and short-term HBV-infected livers containing a comparable amount of human cells. The liver sections also revealed seven red foci consisting of 16 to 43 hepatocytes. In contrast to the picture seen in short-term infection, these red foci were sharply delineated and mildly compressed the surrounding human parenchyma, which indicates that the hepatocytes in these red foci have a growth advantage over the long-term-infected human hepatocytes.

The immunohistochemical staining for HBcAg (Fig. 4C) showed a very intense staining of hepatocyte nuclei and a less intense, but still pronounced staining of cytoplasm and cell surface membranes. The staining for HBsAg (Fig. 4D) showed that the cytoplasm of most hepatocytes contained high amounts of this viral protein. In some hepatocytes with a less intense staining of the cytoplasm, membranous staining became apparent. Overall, the staining intensities were much higher than in the livers of the short-term-infected mice.

Several human hepatic progenitor cells and intermediate hepatocyte-like cells were present not only at the human-mouse parenchymal interface but also within the human parenchymal areas (Fig. 5). This leads to higher numbers of human progenitor and intermediate cells in long-term-infected animals than in short-term or noninfected animals.

Ultrastructural analysis showed that long-term HBV-in-

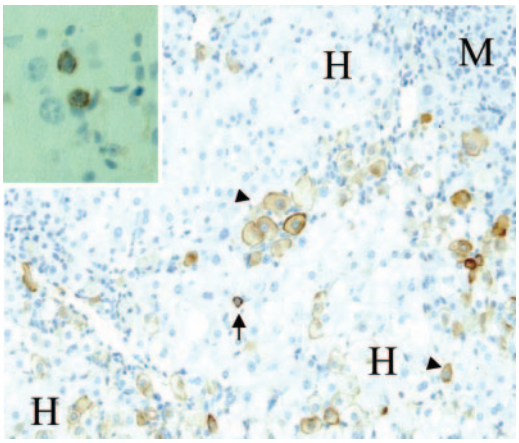

FIG. 5. Immunohistochemistry for human cytokeratin 7 on a liver section from a chimeric mouse long-term infected with HBV. Hepatic progenitor cells (arrows), as well as cells with a phenotype intermediate between progenitors and mature hepatocytes (arrowheads), are not only located at the interface between human (H) and mouse (M) hepatocytes but also within human parenchyma. Staining with anti-cytokeratin 19 confirms the presence of human hepatic progenitor cells (inset). Original magnifications: main image, ×200; inset, ×400.

fected hepatocytes were swollen, ballooned, and considerably damaged. This was never observed in the livers of the short-term-infected mice. The nuclei of most human hepatocytes were completely filled with noncoated round HBV core particles with diameters of 21 to 24 nm. In the cytoplasm of these hepatocytes, nearly all of the cisternae of the endoplasmic reticulum displayed cystic dilations that contained numerous HBsAg tubules and spheres and complete Dane particles (Fig. 6A). Unlike the livers of the short-term-infected and noninfected mice, glycogen granules were scarce in these ballooned human hepatocytes loaded with virus. Human hepatocytes that contained fewer viral particles and showed less cell damage were scarce.

Dysplasia or malignant transformation of human hepatocytes, or tumor cells of the type for which the patient underwent liver surgery were never seen.

Histologic and ultrastructural analysis of liver tissue from a patient with HBV-induced FCH. The needle biopsy and the fragments of the explant liver showed periportal fibrosis with occasional formation of a septum, vague nodularity of the parenchyma, and perisinusoidal fibrosis. The periportal area contained an impressive ductular reaction that extended into

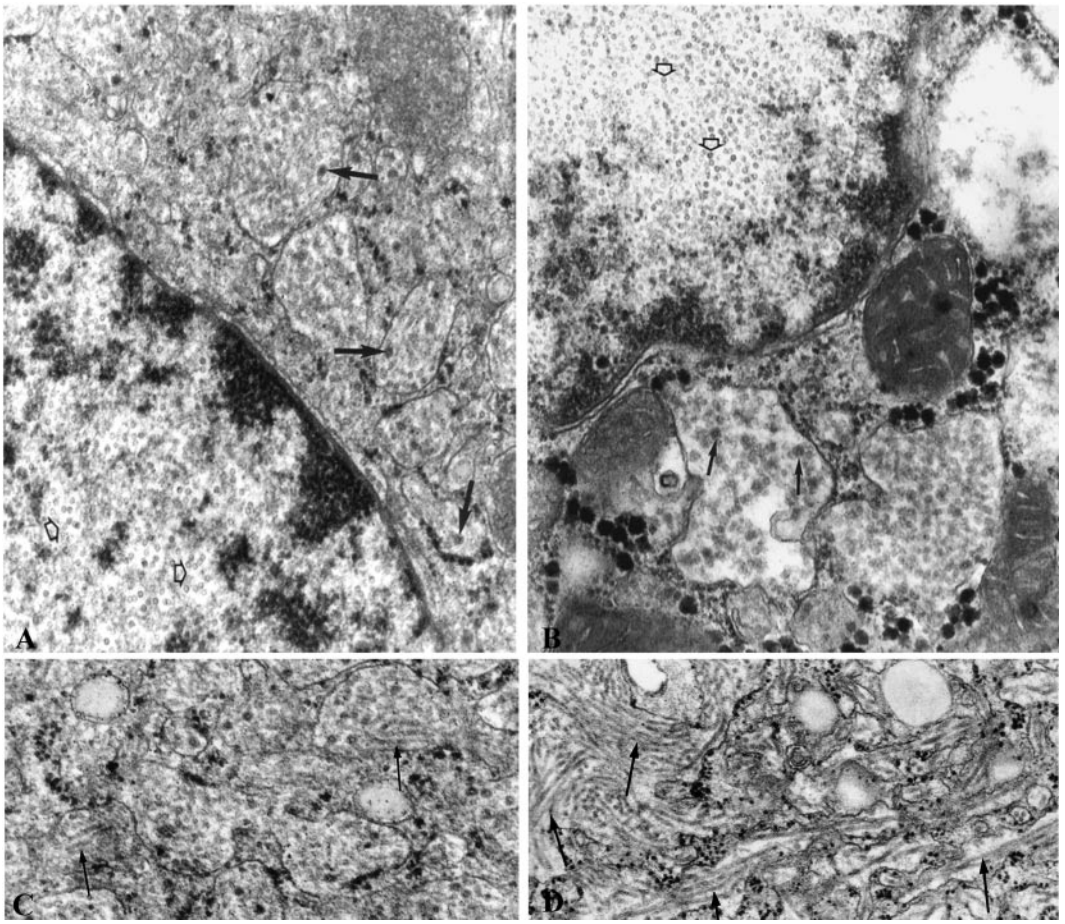

FIG. 6. Electron micrograph of a human hepatocyte in the liver from a long-term-infected chimeric mouse (left) and in the liver of a patient with HBV-induced FCH (right). (A and B) Numerous amounts of HBV core particles (open arrows) are obvious inside the nucleus, whereas complete Dane particles (arrow) are present in the cisternae of the endoplasmic reticulum. (C and D) These cisternae are dilated and contain large amounts of HBV surface tubules. Original magnification: ×77,000.

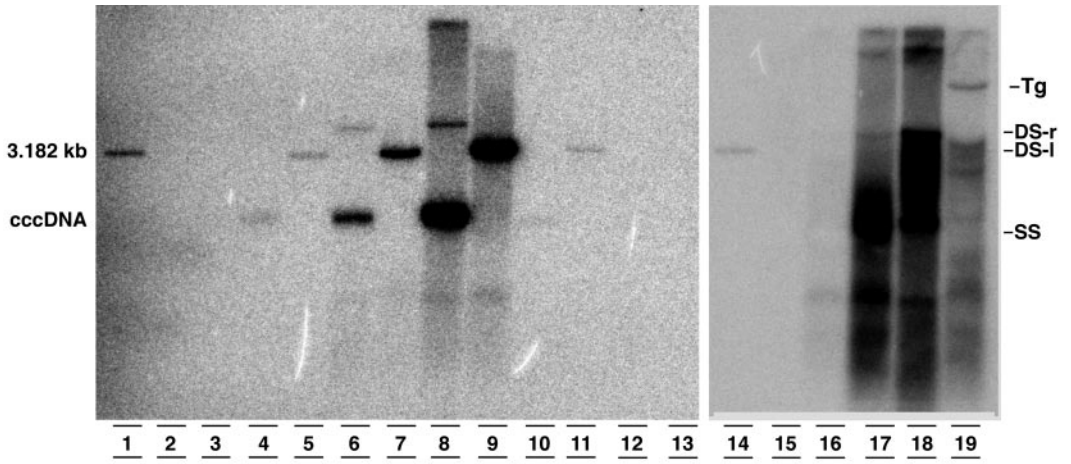

FIG. 7. Southern blot analysis of HBV cccDNA (lanes 2 to 13) and replicative intermediates (lanes 15 to 19) isolated from the livers of a noninfected chimeric mouse (lanes 2, 3, and 15), short-term (lanes 4, 5, and 16) and long-term (lanes 6, 7, and 17) HBV-infected uPA-SCID mice, a patient with HBV-induced FCH (lanes 8, 9, and 18), a chronically HBV-infected chimpanzee (lanes 10 and 11), and an HBV-infected transgenic mouse (lanes 12, 13, and 19). A 3.182-kb molecular weight marker is also included (lanes 1 and 14). After EcoRI digestion, the cccDNA molecules linearized to a double-stranded, linear (DS-l) form (lanes 3, 5, 7, 9, 11, and 13). As expected, cccDNA is not detectable in the HBV transgenic (Tg) mouse extracts. The relative amounts of cccDNA between the different samples cannot be compared because of the varying sizes of the starting material. Replicative intermediates can be easily visualized in the long-term mouse liver but are hardly detectable in the short-term-infected chimeric mouse.

the lobular parenchyma. Singular hepatic progenitor cells and intermediate hepatocyte-like cells were scattered throughout the parenchyma. The parenchyma showed several signs of considerable cell damage and loss: (i) some hepatocytes showed ballooning, (ii) there were numerous ceroid macrophages that sometimes formed clusters, and (iii) a few areas of confluent necrosis were present. The cytoplasm of a considerable proportion of hepatocytes had a "ground-glass" aspect. There was also prominent bilirubinostasis. Bilirubin droplets were present in hepatocytes, bile canaliculi, and frequently in bile ductules with dilated lumina and damaged epithelium. The parenchymal inflammatory infiltrate was only mildly increased.

The immunohistochemical staining for HBcAg (Fig. 4E) showed a very intense staining of nearly all hepatocyte nuclei and a less intense, but still marked, staining of cytoplasm and membrane. The cytoplasm of almost all hepatocytes stained intensely positive for HBsAg (Fig. 4F). Remarkably, some cells from reactive bile ducts were also positive for HBsAg and HBcAg, a feature that has been described previously in chronic HBV infection (13). Striking similarities between the livers of the long-term HBV-infected mice and the human liver with HBV-induced FCH were the presence of extensive hepatocyte damage and loss, the pattern and intensity of immunohistochemical HBV stainings, and the presence of only a mild inflammatory infiltrate.

Ultrastructural evaluation of the small biopsies fixed in glutaraldehyde showed findings almost identical to those seen in the long-term-infected animals (Fig. 6). Many hepatocytes contained nuclei filled with HBV core particles, while the cytoplasmic endoplasmic reticulum cisternae were dilated and packed with HBsAg tubules and spheres and complete Dane particles.

Determination of HBV cccDNA, DNA, and RNA. The livers of one short-term-infected and one long-term-infected animal were also analyzed for the presence of HBV cccDNA, replicative intermediates, and RNA transcripts. Using Southern blotting, cccDNA could easily be identified in both chimeric livers (Fig. 7A). After EcoRI digestion, the cccDNA molecules were linearized and comigrated with the linear HBV DNA present in the total DNA isolated from the same tissue. cccDNA could also be detected in liver biopsies from a chronically infected chimpanzee and the FCH patient, but was absent in DNA extracts from HBV transgenic mice. HBV DNA replicative intermediates were detected in all liver samples except in the noninfected chimeric mouse (Fig. 7B). The cccDNA copy number per infected hepatocyte was quantified by using quantitative real-time PCR. In the liver of a short-term-infected animal we detected 1.4 cccDNA molecules per $HBcAg^+$ human hepatocyte. In contrast, in the long-term-infected animal the amount of cccDNA molecules per HBV-infected human hepatocyte increased to 65.7 copies/cell. The liver of the FCH patient contained 6.8 cccDNA molecules per hepatocyte.

Northern blot analysis showed very high HBV gene expression in the long-term mouse liver but only low expression in the chimeric mouse liver after 21 days (Fig. 8). The preS1 mRNA was visible only in the liver extracts of the long-term-infected chimeric uPA-mouse and in the HBV transgenic mouse.

DISCUSSION

The hepatic injury during acute and chronic HBV infections is thought to be caused by the host's immune response against the infected hepatocytes (6). However, in some severely immunosuppressed chronic HBV patients, excessive viremia and a very severe, sometimes fatal hepatic disease, known as FCH may occur. This suggests that severe liver pathology may arise in the absence of a functional immune system (5, 27, 39, 43). To examine the pathology induced by HBV in an immune deficient host, we have infected chimeric human liver-uPA-SCID mice with HBV.

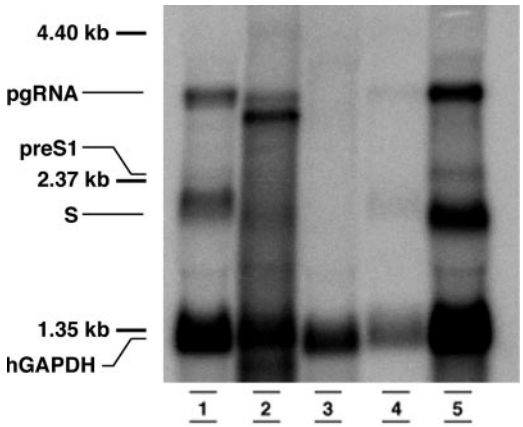

FIG. 8. Northern blot analysis of total RNA extracts of the livers of an HBV-transgenic mouse (lane 1), a patient with HBV-induced FCH (lane 2), a noninfected chimeric mouse (lane 3), a short-term HBV-infected mouse (lane 4), and a long-term HBV-infected mouse (lane 5). From each sample 10 μg of total RNA was loaded. The Pre-S1 transcript can be easily seen in the long-term-infected chimeric mouse. The lower hGAPDH signal in the short-term-infected mouse reflects a lower amount of human hepatocytes present in the chimeric liver.

At several moments after infection, the concentrations of HBsAg, HBeAg, and HBV DNA in mouse plasma were determined. In agreement with Degushi et al. (12) and previous observations of our lab (54), very strong linear correlations between HBsAg and HBeAg and HBV DNA were observed. Also, a linear correlation between the amount of HBeAg and HBV DNA was seen. Two groups that independently analyzed serum from chronic HBV patients were unable to find such a relationship before the start of antiviral treatment (4, 25). However, during antiviral treatment, these researchers found a correlation between HBeAg and HBV DNA levels and concluded that quantification of HBeAg in serum or plasma may be a valuable alternative to HBV DNA measurements to monitor the success of antiviral treatment.

Compared to noninfected human liver-uPA-SCID mice, HBV-infected animals have a decreased life expectancy and their premature death is caused by the progressive deterioration of the liver structure and function. Several observations are indicative of a direct cytopathic effect of the hepatitis B virus in our model. A large proportion of human hepatocytes in long-term-infected animals acquired a ground-glass appearance. This was not seen in noninfected or short-term-infected mice. These ground-glass hepatocytes stained extremely positive for both HBsAg and HBcAg, whereas the staining pattern of short-term-infected hepatocytes was less pronounced. Electron microscopic analysis revealed several signs of structural damage within the infected human hepatocytes. Large numbers of clustering ceroid macrophages were only observed in the human areas of the livers of long-term-infected animals. This is a hallmark of ongoing cell death and the ensuing removal of cellular remnants. The physical condition and functional integrity of the long-term-infected hepatocytes were irreversibly compromised, since these cells produced less albumin and were literally pushed aside by regenerative mouse "red nodules." These regenerative mouse red nodules do not cause the death of the human hepatocytes by themsleves. Sandgren et al. showed that somatic deletion of the uPA-transgene results in a restoration of the normal liver architecture (53). If these nodules were just replacing the human hepatocytes then the clinical condition of our infected mice would ameliorate and the animals would be rescued. However, this is not happening. The overwhelming infection and replication of HBV in human hepatocytes causes massive dysfunction of these cells that cannot be compensated for sufficiently by the "healthy" mouse hepatocytes in the red nodules. This process ultimately leads to liver failure and death of the animals. Only one animal survived the HBV infection and showed signs of clinical improvement. In the liver of this animal lower amounts of human hepatocytes were present, whereas large amounts of healthy, regenerative mouse hepatocytes were observed. These red nodules most likely rescued this animal.

Dandri et al. (9) were the first to successfully infect chimeric immune deficient uPA mice with HBV. These researchers did not report HBV-induced hepatocellular toxicity in two infected animals. Some important differences in the experimental design may explain this. The human hepatocytes were transplanted into heterozygous $uPA^{+/-}$ mice and not in homozygous $uPA^{+/+}$ animals like we did. The transfer of hepatocytes in heterozygous mice results in a repopulation grade with human cells of only 2 to 10%, meaning that most of the liver parenchyma is occupied by healthy mouse hepatocytes derived from $uPA^{-/-}$ revertants. A lethal effect of HBV infection cannot be observed since these mice even survive without a hepatocyte graft. In addition, the infected animals were sacrificed 8 weeks after transplantation, which may have been to soon to observe the cytopathic effects we report here. At that moment, the animals had high levels of HBV DNA and HBV proteins in their plasma and a strong nuclear expression of the HBV core protein in the liver, phenomena we also observed at a similar time point. Levels of circulating HBV DNA with values exceeding 10^9 copies/ml are also common in immunosuppressed HBV patients (1, 28).

Tsuge et al. recently described long-term HBV infection in uPA-SCID mice (57). Several weeks after infection, the concentration of human albumin decreased in these animals, albeit less dramatically than what we observed. It is not clear whether this is due to the HBV infection or to a spontaneous loss of chimerism. Obvious signs of a cytopathic effect were not reported, and a lethal effect is less likely in this setup because the low levels of human albumin suggest the presence of high amounts of regenerative red nodules. These would rescue the animals in case of graft failure.

$uPA^{+/-}$ $RAG2^{-/-}$ mice transplanted with tupaia hepatocytes have also been infected with HBV (10). In these animals the HBV infection persisted for 6 months, the experimental endpoint, and no signs of hepatocellular damage were reported. The main differences with the human liver-uPA model are that the onset of viremia was considerably delayed and that the plasma levels of HBV DNA were significantly lower. This may be due to the nature of the tupaia hepatocytes.

Similarly, hepatocytes from a woodchuck infected with the woodchuck hepatitis virus were transplanted in uPA-RAG2 mice. These animals experienced high viremia for more than 10 months without obvious lesions in the liver. It might be that the woodchuck hepatitis virus is less cytopathic than HBV.

Alternatively, this difference may also be related to the different nature of the woodchuck hepatocytes.

Our observations closely resemble those made by Lenhoff et al. in a model for the study of the duck hepatitis B virus (34). Three-day-old ducklings were infected with a duck hepatitis B virus strain that contained a mutation in the Pre-S region. This mutation induced elevated levels of viral cccDNA and viral capsid protein in the nucleus of the infected hepatocytes. In addition to high intracellular viral protein expression, we also observed a 47-fold increase in cccDNA copy number per infected hepatocyte when we compared the short- and long-term-infected animals.

The infected ducklings also displayed high viremia and hepatocellular damage. Like in our model, this cell damage elicited an increase of mononuclear cells and regenerating bile ductule-like cells in the liver parenchyma. In biopsies of patients with chronic viral hepatitis, the number of hepatic progenitor cells is also correlated with the severity of hepatocyte damage and loss (18). As a consequence of the cytopathic effect, the ducklings experienced a marked growth retardation. In contrast to our study, this cytopathic effect lasted for only 23 days, and the recovery was associated with the appearance of a noncytopathic revertant virus (35). We did not observe any sequence variability during the 88-day infection period.

The mechanisms underlying the cytopathic effect of the virus have not yet been defined. Several in vitro and in vivo studies showed that the accumulation of the L protein leads to the appearance of ground-glass hepatocytes (7, 17) and can induce stress in the endoplasmic reticulum (58), as well as oxidative DNA damage and mutagenesis (26). The virus isolate we used here lacked the mutations in the pre-S region that have been shown to lead to the development of ground-glass hepatocytes in chronic carriers (16, 45, 61). It can be argued that the cytopathic effect seen in the present study is the result of the human hepatocytes being infected with an isolate that has mutations in the basic core promoter. However, these mutations have also be found in asymptomatic carriers, in patients experiencing only a mild form of chronic HBV infection (19, 31, 48, 55), and in immune compromised HBV patients with no or mild liver disease (23, 44, 50).

In the context of the present study, an ultrastructural analysis on biopsies from a FCH liver has been performed for the first time. This evaluation revealed massive amounts of viral and subviral particles inside ballooned and damaged hepatocytes. Electron micrographs of human hepatocytes in the long-term-infected mice could not be distinguished from those of the FCH liver. We did not detect a significant increase in cccDNA copy number in the FCH patient, indicating that the cause of the cytopathic effect might be different at the molecular level.

Our data and the clinicopathological observations made in other patients with FCH suggest that, in the absence of a functioning immune system as it occurs in SCID mice and severely immunosuppressed patients, HBV can replicate and express its proteins in an unrestrained fashion. This leads to excessive accumulation of viral proteins, cell damage, and ultimately cell death. Our mouse model can be useful for studying new therapies and strategies to control the viral replication during immunosuppression after organ transplantation in patients with chronic hepatitis B infection. It may also be useful for the evaluation and prediction of the pathogenic effect of the various genotypes of HBV and certain HBV mutants.

ACKNOWLEDGMENTS

We thank S. Couvent and F. Clinckspoor for the serologic analysis of the mouse plasma. We also want to thank Francis Chisari for critically reading the manuscript and providing helpful assistance and advice.

This research was supported by the Special Research Fund of Ghent University (BOF), by a doctoral grant for P.M. (011D3099), and by a Concerted Action Grant (no. 12050203). S.W. was supported by National Institutes of Health grant R01-AI20001, and L.L. is a postdoctoral researcher of the Research Foundation Flanders.

REFERENCES

1. **Altfeld, M., J. K. Rockstroh, M. Addo, B. Kupfer, I. Pult, H. Will, and U. Spengler.** 1998. Reactivation of hepatitis B in a long-term anti-HBs-positive patient with AIDS following lamivudine withdrawal. J. Hepatol. **29:**306–309.
2. **Bancroft, J., and H. Cook.** 1984. Manual of histological techniques. Churchill Livingstone, Edinburgh, United Kingdom.
3. **Benner, K. G., R. G. Lee, E. B. Keeffe, R. R. Lopez, A. W. Sasaki, and C. W. Pinson.** 1992. Fibrosing cytolytic liver failure secondary to recurrent hepatitis B after liver transplantation. Gastroenterology **103:**1307–1312.
4. **Bernard, F., G. Raymond, B. Willems, and J. P. Villeneuve.** 1997. Quantitative assessment of serum hepatitis B e antigen, IgM hepatitis B core antibody and HBV DNA in monitoring the response to treatment in patients with chronic hepatitis B. J. Viral Hepat. **4:**265–272.
5. **Chen, C. H., P. J. Chen, J. S. Chu, K. H. Yeh, M. Y. Lai, and D. S. Chen.** 1994. Fibrosing cholestatic hepatitis in a hepatitis B surface antigen carrier after renal transplantation. Gastroenterology **107:**1514–1518.
6. **Chisari, F. V., and C. Ferrari.** 1995. Hepatitis B virus immunopathogenesis. Annu. Rev. Immunol. **13:**29–60.
7. **Chisari, F. V., P. Filippi, J. Buras, A. McLachlan, H. Popper, C. A. Pinkert, R. D. Palmiter, and R. L. Brinster.** 1987. Structural and pathological effects of synthesis of hepatitis B virus large envelope polypeptide in transgenic mice. Proc. Natl. Acad. Sci. USA **84:**6909–6913.
8. **Chomczynski, P., and N. Sacchi.** 1987. Single-step method of RNA isolation by acid guanidinium thiocyanate-phenol-chloroform extraction. Anal. Biochem. **162:**156–159.
9. **Dandri, M., M. R. Burda, E. Torok, J. M. Pollok, A. Iwanska, G. Sommer, X. Rogiers, C. E. Rogler, S. Gupta, H. Will, H. Greten, and J. Petersen.** 2001. Repopulation of mouse liver with human hepatocytes and in vivo infection with hepatitis B virus. Hepatology **33:**981–988.
10. **Dandri, M., M. R. Burda, D. M. Zuckerman, K. Wursthorn, U. Matschl, J. M. Pollok, X. Rogiers, A. Gocht, J. Kock, H. E. Blum, F. von Weizsacker, and J. Petersen.** 2005. Chronic infection with hepatitis B viruses and antiviral drug evaluation in uPA mice after liver repopulation with tupaia hepatocytes. J. Hepatol. **42:**54–60.
11. **Davies, S. E., B. C. Portmann, J. G. O'Grady, P. M. Aldis, K. Chaggar, G. J. Alexander, and R. Williams.** 1991. Hepatic histological findings after transplantation for chronic hepatitis B virus infection, including a unique pattern of fibrosing cholestatic hepatitis. Hepatology **13:**150–157.
12. **Deguchi, M., N. Yamashita, M. Kagita, S. Asari, Y. Iwatani, T. Tsuchida, K. Iinuma, and I. K. Mushahwar.** 2004. Quantitation of hepatitis B surface antigen by an automated chemiluminescent microparticle immunoassay. J. Virol. Methods **115:**217–222.
13. **Delladetsima, J. K., I. Vafiadis, N. C. Tassopoulos, V. Kyriakou, A. Apostolaki, and T. Smyrnoff.** 1994. HBcAg and HBsAg expression in ductular cells in chronic hepatitis B. Liver **14:**71–75.
14. **Desmet, V. J.** 2003. Liver tissue examination. J. Hepatol. **39**(Suppl. 1)**:**S43–S49.
15. **Desmet, V. J., P. Van Eyken, and R. Sciot.** 1990. Cytokeratins for probing cell lineage relationships in developing liver. Hepatology **12:**1249–1251.
16. **Fan, Y. F., C. C. Lu, W. C. Chen, W. J. Yao, H. C. Wang, T. T. Chang, H. Y. Lei, A. L. Shiau, and I. J. Su.** 2001. Prevalence and significance of hepatitis B virus (HBV) pre-S mutants in serum and liver at different replicative stages of chronic HBV infection. Hepatology **33:**277–286.
17. **Foo, N. C., B. Y. Ahn, X. Ma, W. Hyun, and T. S. Yen.** 2002. Cellular vacuolization and apoptosis induced by hepatitis B virus large surface protein. Hepatology **36:**1400–1407.
18. **Fotiadu, A., V. Tzioufa, E. Vrettou, D. Koufogiannis, C. S. Papadimitriou, and P. Hytiroglou.** 2004. Progenitor cell activation in chronic viralhepatitis. Liver Int. **24:**268–274.
19. **Gandhe, S. S., M. S. Chadha, A. M. Walimbe, and V. A. Arankalle.** 2003. Hepatitis B virus: prevalence of precore/core promoter mutants in different clinical categories of Indian patients. J. Viral Hepat. **10:**367–382.
20. **Gerdes, J., U. Schwab, H. Lemke, and H. Stein.** 1983. Production of a mouse monoclonal antibody reactive with a human nuclear antigen associated with cell proliferation. Int. J. Cancer **31:**13–20.

21. **Guidotti, L. G., B. Matzke, H. Schaller, and F. V. Chisari.** 1995. High-level hepatitis B virus replication in transgenic mice. J. Virol. **69:**6158–6169.
22. **Guidotti, L. G., R. Rochford, J. Chung, M. Shapiro, R. Purcell, and F. V. Chisari.** 1999. Viral clearance without destruction of infected cells during acute HBV infection. Science **284:**825–829.
23. **Gunther, S., N. Piwon, A. Iwanska, R. Schilling, H. Meisel, and H. Will.** 1996. Type, prevalence, and significance of core promoter/enhancer II mutations in hepatitis B viruses from immunosuppressed patients with severe liver disease. J. Virol. **70:**8318–8331.
24. **Heckel, J. L., E. P. Sandgren, J. L. Degen, R. D. Palmiter, and R. L. Brinster.** 1990. Neonatal bleeding in transgenic mice expressing urokinase-type plasminogen activator. Cell **62:**447–456.
25. **Heijtink, R. A., J. Kruining, P. Honkoop, M. C. Kuhns, W. C. Hop, A. D. Osterhaus, and S. W. Schalm.** 1997. Serum HBeAg quantitation during antiviral therapy for chronic hepatitis B. J. Med. Virol. **53:**282–287.
26. **Hsieh, Y. H., I. J. Su, H. C. Wang, W. W. Chang, H. Y. Lei, M. D. Lai, W. T. Chang, and W. Huang.** 2004. Pre-S mutant surface antigens in chronic hepatitis B virus infection induce oxidative stress and DNA damage. Carcinogenesis **25:**2023–2032.
27. **Hung, Y. B., J. T. Liang, J. S. Chu, K. M. Chen, and C. S. Lee.** 1995. Fulminant hepatic failure in a renal transplant recipient with positive hepatitis B surface antigens: a case report of fibrosing cholestatic hepatitis. Hepatogastroenterology **42:**913–918.
28. **Jung, S., H. C. Lee, J. M. Han, Y. J. Lee, Y. H. Chung, Y. S. Lee, Y. Kwon, E. Yu, and D. J. Suh.** 2002. Four cases of hepatitis B virus-related fibrosing cholestatic hepatitis treated with lamivudine. J. Gastroenterol. Hepatol. **17:** 345–350.
29. **Kimbi, G. C., A. Kramvis, and M. C. Kew.** 2004. Distinctive sequence characteristics of subgenotype A1 isolates of hepatitis B virus from South Africa. J. Gen. Virol. **85:**1211–1220.
30. **Krucken, J., R. M. Schroetel, I. U. Muller, N. Saidani, P. Marinovski, W. P. Benten, O. Stamm, and F. Wunderlich.** 2004. Comparative analysis of the human gimap gene cluster encoding a novel GTPase family. Gene **341:**291–304.
31. **Kurosaki, M., N. Enomoto, Y. Asahina, I. Sakuma, T. Ikeda, S. Tozuka, N. Izumi, F. Marumo, and C. Sato.** 1996. Mutations in the core promoter region of hepatitis B virus in patients with chronic hepatitis B. J. Med. Virol. **49:**115–123.
32. **Lau, J. Y., V. G. Bain, S. E. Davies, J. G. O'Grady, A. Alberti, G. J. Alexander, and R. Williams.** 1992. High-level expression of hepatitis B viral antigens in fibrosing cholestatic hepatitis. Gastroenterology **102:**956–962.
33. **Lau, S. K., S. Prakash, S. A. Geller, and R. Alsabeh.** 2002. Comparative immunohistochemical profile of hepatocellular carcinoma, cholangiocarcinoma, and metastatic adenocarcinoma. Hum. Pathol. **33:**1175–1181.
34. **Lenhoff, R. J., C. A. Luscombe, and J. Summers.** 1999. Acute liver injury following infection with a cytopathic strain of duck hepatitis B virus. Hepatology **29:**563–571.
35. **Lenhoff, R. J., C. A. Luscombe, and J. Summers.** 1998. Competition in vivo between a cytopathic variant and a wild-type duck hepatitis B virus. Virology **251:**85–95.
36. **Libbrecht, L., L. Meerman, F. Kuipers, T. Roskams, V. Desmet, and P. Jansen.** 2003. Liver pathology and hepatocarcinogenesis in a long-term mouse model of erythropoietic protoporphyria. J. Pathol. **199:**191–200.
37. **Libbrecht, L., and T. Roskams.** 2002. Hepatic progenitor cells in human liver diseases. Semin. Cell Dev. Biol. **13:**389–396.
38. **Lindh, M., A. S. Andersson, and A. Gusdal.** 1997. Genotypes, nt 1858 variants, and geographic origin of hepatitis B virus: large-scale analysis using a new genotyping method. J. Infect. Dis. **175:**1285–1293.
39. **Lok, A. S., R. H. Liang, E. K. Chiu, K. L. Wong, T. K. Chan, and D. Todd.** 1991. Reactivation of hepatitis B virus replication in patients receiving cytotoxic therapy: report of a prospective study. Gastroenterology **100:**182–188.
40. **Luna, L.** 1968. Manual of histologic staining methods of the Armed Forces Institute of Pathology, 3rd ed. McGraw-Hill Book Company, New York, N.Y.
41. **MacSween, R.** 2002. Morphological diagnostic procedure: liver biopsy, fine needle aspiration biopsy, p. 943–960. *In* P. Antony (ed.), Pathology of the liver. Churchill Livingstone, Edinburgh, United Kingdom.
42. **Mason, A. L., M. Wick, H. M. White, K. G. Benner, R. G. Lee, F. Regenstein, C. A. Riely, V. G. Bain, C. Campbell, and R. P. Perrillo.** 1993. Increased hepatocyte expression of hepatitis B virus transcription in patients with features of fibrosing cholestatic hepatitis. Gastroenterology **105:**237–244.
43. **McIvor, C., J. Morton, A. Bryant, W. G. Cooksley, S. Durrant, and N. Walker.** 1994. Fatal reactivation of precore mutant hepatitis B virus associated with fibrosing cholestatic hepatitis after bone marrow transplantation. Ann. Intern. Med. **121:**274–275.
44. **McMillan, J. S., D. S. Bowden, P. W. Angus, G. W. McCaughan, and S. A. Locarnini.** 1996. Mutations in the hepatitis B virus precore/core gene and core promoter in patients with severe recurrent disease following liver transplantation. Hepatology **24:**1371–1378.
45. **Melegari, M., P. P. Scaglioni, and J. R. Wands.** 1997. The small envelope protein is required for secretion of a naturally occurring hepatitis B virus mutant with pre-S1 deleted. J. Virol. **71:**5449–5454.
46. **Meuleman, P., L. Libbrecht, R. De Vos, B. de Hemptinne, K. Gevaert, J. Vandekerckhove, T. Roskams, and G. Leroux-Roels.** 2005. Morphological and biochemical characterization of a human liver in a uPA-SCID mouse chimera. Hepatology **41:**847–856.
47. **Meuleman, P., P. Vanlandschoot, and G. Leroux-Roels.** 2003. A simple and rapid method to determine the zygosity of uPA-transgenic SCID mice. Biochem. Biophys. Res. Commun. **308:**375–378.
48. **Nishizono, A., M. Hiraga, K. Kohno, Y. T. Sonoda, H. Terao, T. Fujioka, M. Nasu, and K. Mifune.** 1995. Mutations in the core promoter/enhancer II regions of naturally occurring hepatitis B virus variants and analysis of the effects on transcription activities. Intervirology **38:**290–294.
49. **Owiredu, W. K., A. Kramvis, and M. C. Kew.** 2001. Hepatitis B virus DNA in serum of healthy black African adults positive for hepatitis B surface antibody alone: possible association with recombination between genotypes A and D. J. Med. Virol. **64:**441–454.
50. **Preikschat, P., S. Gunther, S. Reinhold, H. Will, K. Budde, H. H. Neumayer, D. H. Kruger, and H. Meisel.** 2002. Complex HBV populations with mutations in core promoter, C gene, and pre-S region are associated with development of cirrhosis in long-term renal transplant recipients. Hepatology **35:**466–477.
51. **Rhim, J. A., E. P. Sandgren, J. L. Degen, R. D. Palmiter, and R. L. Brinster.** 1994. Replacement of diseased mouse liver by hepatic cell transplantation. Science **263:**1149–1152.
52. **Rhim, J. A., E. P. Sandgren, R. D. Palmiter, and R. L. Brinster.** 1995. Complete reconstitution of mouse liver with xenogeneic hepatocytes. Proc. Natl. Acad. Sci. USA **92:**4942–4946.
53. **Sandgren, E. P., R. D. Palmiter, J. L. Heckel, C. C. Daugherty, R. L. Brinster, and J. L. Degen.** 1991. Complete hepatic regeneration after somatic deletion of an albumin-plasminogen activator transgene. Cell **66:**245–256.
54. **Steyaert, S., P. Vanlandschoot, H. Van Vlierberghe, H. Diepolder, and G. Leroux-Roels.** 2003. Soluble CD14 levels are increased and inversely correlated with the levels of hepatitis B surface antigen in chronic hepatitis B patients. J. Med. Virol. **71:**188–194.
55. **Takahashi, K., K. Aoyama, N. Ohno, K. Iwata, Y. Akahane, K. Baba, H. Yoshizawa, and S. Mishiro.** 1995. The precore/core promoter mutant (T1762A1764) of hepatitis B virus: clinical significance and an easy method for detection. J. Gen. Virol. **76**(Pt. 12)**:**3159–3164.
56. **Thimme, R., S. Wieland, C. Steiger, J. Ghrayeb, K. A. Reimann, R. H. Purcell, and F. V. Chisari.** 2003. $CD8^+$ T cells mediate viral clearance and disease pathogenesis during acute hepatitis B virus infection. J. Virol. **77:** 68–76.
57. **Tsuge, M., N. Hiraga, H. Takaishi, C. Noguchi, H. Oga, M. Imamura, S. Takahashi, E. Iwao, Y. Fujimoto, H. Ochi, K. Chayama, C. Tateno, and K. Yoshizato.** 2005. Infection of human hepatocyte chimeric mouse with genetically engineered hepatitis B virus. Hepatology **42:**1046–1054.
58. **Wang, H. C., H. C. Wu, C. F. Chen, N. Fausto, H. Y. Lei, and I. J. Su.** 2003. Different types of ground glass hepatocytes in chronic hepatitis B virus infection contain specific pre-S mutants that may induce endoplasmic reticulum stress. Am. J. Pathol. **163:**2441–2449.
59. **Wennerberg, A. E., M. A. Nalesnik, and W. B. Coleman.** 1993. Hepatocyte paraffin 1: a monoclonal antibody that reacts with hepatocytes and can be used for differential diagnosis of hepatic tumors. Am. J. Pathol. **143:**1050–1054.
60. **Wieland, S. F., H. C. Spangenberg, R. Thimme, R. H. Purcell, and F. V. Chisari.** 2004. Expansion and contraction of the hepatitis B virus transcriptional template in infected chimpanzees. Proc. Natl. Acad. Sci. USA **101:** 2129–2134.
61. **Xu, Z., and T. S. Yen.** 1996. Intracellular retention of surface protein by a hepatitis B virus mutant that releases virion particles. J. Virol. **70:**133–140.
62. **Zanati, S. A., S. A. Locarnini, J. P. Dowling, P. W. Angus, F. J. Dudley, and S. K. Roberts.** 2004. Hepatic failure due to fibrosing cholestatic hepatitis in a patient with pre-surface mutant hepatitis B virus and mixed connective tissue disease treated with prednisolone and chloroquine. J. Clin. Virol. **31:**53–57.